AGU PUBLICATIONS

Radio Science

RESEARCH ARTICLE
10.1002/2015RS005865

Key Points:
- Characterization of interfade duration is mandatory when designing fade impairment mitigation techniques
- At least 3 years of measurements is needed to characterize the interfade events
- There is a high demand for a quick response on recovering after a fade event

Correspondence to:
F. Jorge,
flaviojorge@ua.pt

Citation:
Jorge, F., C. Riva, and A. Rocha (2016), Characterization of interfade duration for satellite communication systems design and optimization in a temperate climate, *Radio Sci.*, *51*, 150–159, doi:10.1002/2015RS005865.

Received 20 NOV 2015
Accepted 19 FEB 2016
Accepted article online 26 FEB 2016
Published online 14 MAR 2016

Characterization of interfade duration for satellite communication systems design and optimization in a temperate climate

Flávio Jorge[1], Carlo Riva[2], and Armando Rocha[1]

[1]Instituto de Telecomunicações e Departamento de Electrónica, Telecomunicações e Informática, Universidade de Aveiro, Aveiro, Portugal, [2]DEIB/Politecnico di Milano - IEIIT/CNR, Milano, Italy

Abstract The characterization of the fade dynamics on Earth-satellite links is an important subject when designing the so called *fade mitigation techniques* that contribute to the proper reliability of the satellite communication systems and the customers' quality of service (QoS). The interfade duration, defined as the period between two consecutive fade events, has been only poorly analyzed using limited data sets, but its complete characterization would enable the design and optimization of the satellite communication systems by estimating the system requirements to recover in time before the next propagation impairment. Depending on this analysis, several actions can be taken ensuring the service maintenance. In this paper we present for the first time a detailed and comprehensive analysis of the interfade events statistical properties based on 9 years of in-excess attenuation measurements at Ka band (19.7 GHz) with very high availability that is required to build a reliable data set mainly for the longer interfade duration events. The number of years necessary to reach the statistical stability of interfade duration is also evaluated for the first time, providing a reference when accessing the relevance of the results published in the past. The study is carried out in Aveiro, Portugal, which is conditioned by temperate Mediterranean climate with Oceanic influences.

1. Introduction

Among the propagation constraints impairing the satellite communication systems, the attenuation assumes a central role on the system reliability and quality of service (QoS) as perceived by customers, once it is responsible for degrading the transmitted signal. In order to ensure a proper QoS, understood as the delivered service availability and bandwidth, the traditional approach consists on applying a static attenuation margin, obtained from long-term attenuation statistics, to comply with the service-contracted specifications. However, when delivering satellite services at higher-frequency bands, such as the Ka and the Q/V bands, the traditional approach no longer is able, by itself, to ensure the system reliability, not only due to transmission power constraints (associated to the limited resources on board of the satellite and induced system interference) but also due to the increased severity of the propagation phenomena. Several fade mitigation techniques (FMTs) have been exploited in order to overcome the above referred constraints. For example, site diversity is a technique which exploits the spatial propagation channel correlation by switching the traffic to another ground station, far from the first, and establishing a new link which is, from the propagation channel point of view, poorly correlated to the previous one [*Luglio et al*., 2002]. On the other hand, for non-real-time services or for those allowing a short recovering time, the temporal propagation channel correlation can be exploited by means of storing the information during the unavailable period to be transmitted later on through the same link as proposed by *Braten et al*. [2001], a FMT known as time diversity. Among many others, the dynamic allocation of power, by means of beamforming, i.e., assigning the antenna radiation pattern, accordingly to the users' needs and the propagation channel conditions also allows an improved performance of the satellite system, which is absolutely essential when considering satellite commercial competitive services [*Paraboni et al*., 2002, 2009; *Nebuloni et al*., 2013]. The design of such FMTs requires the characterization of the fade dynamics aspects, such as fade duration, fade slope, and interfade duration [*Timothy et al*., 2000; *Amaya and Rogers*, 2003; *Anon*, 2005, P.1623-1; *Amaya and Nguyen*, 2005; *Castanet and Van de Kamp*, 2003; *Arnold et al*., 1982] which further contribute to identify the underlying physical mechanisms that, of course, are important for the modeling of the associated propagation phenomena [*Timothy et al*., 1998].

The interfade duration is one aspect of the fade dynamics of great importance. If on one hand the fade duration enables the prediction of a time interval during which a fade occurs, and so during which fade

countermeasurements must be applied, on the other hand the interfade duration enables the prediction of the time interval during which the satellite system has the opportunity to recover from the previous impairment. For example, if the probability of having interfade events of short duration is high, then services having long holding times can be compromised [*Arnold et al*., 1982]. When designing these systems, it is necessary to have information regarding the interfade duration statistical properties once it provides valuable information to the decision support systems, answering questions like "is it worth it to switch to the previous ground station or is it expectable to have to switch to this same link shortly?" in case of using site diversity, "is the available time, between two consecutive fades, long enough to transmit the buffered data without interruption or can the frequent system unavailability cause the overflow of data buffers?" if a time diversity scheme is under consideration, or in case of applying beamforming, "is it possible to sustain this power distribution or another FMT is required?"

Interfade events can be characterized by means of either the conditional complementary cumulative distribution function (CCCDF) of interfade duration, i.e., the probability of not exceeding a given attenuation threshold in periods longer than a certain duration, or the CCCDF of the number of interfade durations, i.e., the number of interfade events exceeding a certain duration for a given attenuation threshold. All of these attempts were based on limited interfade duration and/or on low availability measurement data sets, leading to a poor statistical characterization.

Arnold et al. [1982] presented 2 years of interfade measurements at 19.04 GHz collected at the Bell Laboratories in Crawford Hill during a campaign using the COMSTAR satellite. The data were collected with a sampling rate of one sample every 30 s and with an amplitude accuracy of about 0.5 dB. Based on the CCCDF of the number of interfade events per year, they found that the slope of the distribution decreases with the attenuation threshold, whereas the median interfade duration increases. Moreover the higher attenuation events were more isolated: almost 80% of the 40 dB attenuation events were separated by more than 2 h, to be compared with the 35% of the 5 dB events. From similar statistics measured at 11.2 GHz in Singapore, *Timothy et al*. [2000] concluded that the interfade duration for half of the rain events in a year is less than 10 min.

Braten et al. [2001] presented a CCCDF for 1 year of fade and interfade duration measurements carried out in Ottawa during the NASA campaign with ACTS satellite at 20.2 GHz in order to estimate the system availability: after a fade event of at least 10 s the system was declared as unavailable, whereas after an interfade event of at least 10 s the system was declared available again, which is a reference time for recovering communication after deep fade events. Some additional data on this topic, collected as well with the ACTS satellite, are presented in *Braten and Amaya* [2000] where also some difficulties with the measurement equipment are reported.

In *Castanet and Van de Kamp* [2003] CCCDFs of interfade duration were presented using measurements at 20 and 30 GHz during the Olympus campaign in Denmark. The importance of interfade duration is stressed, but the experimental statistical data are not commented.

Pan and Allnutt [2004] presented the annual and seasonal average duration of interfade events measured during 4 years at 12.75 GHz in Papua New Guinea for several attenuation thresholds, but no further discussion is detailed.

Based on 3 years of interfade duration measurements carried out in Belgium during the Olympus campaign at 30 GHz, *Amaya and Nguyen* [2005] presented both the CCCDF of interfade duration and of the number of interfade events. The impact on distributions by filtering the data was found to be negligible for durations exceeding 30–50 s. The number of interfade events for a certain duration decreases with the attenuation threshold, a tendency which is reversed for very long periods. The probability distribution, which depends on the attenuation threshold, is generally lognormal. Similar conclusions were drawn by *Amaya and Rogers* [2003] using 4 years of interfade duration measurements with ACTS satellite at 30 GHz in Canada.

Using 1 year of data collected at 50GHz, *Garcia-del-Pino et al*. [2011] confirmed that short interfade durations (less than 10 s), mainly due to scintillation, follow a power law distribution, while medium and long interfade durations, mainly related to precipitation, follow a lognormal one.

The following sections provide for the first time a comprehensive, exhaustive, and critical analysis on interfade duration based on a database comprising 9 years of measurements with very high availability. The number of years necessary to reach a statistical stability for the interfade duration is also evaluated, which impacts

Table 1. Experimental Setup

Satellite Name	Eutelsat 13A
Satellite orbital position (°E)	13
Frequency (GHz)	19.7
Elevation angle (deg)	38
Polarization	linear horizontal
Polarization tilt angle (deg)	23
Earth station latitude (°N)	40.63
Earth station longitude (°W)	8.66
Earth station altitude above mean sea level (m)	18

the evaluation of the relevance of the few results published in the past. As long as interfade models still have not been published as comprehensive statistics are not available in the literature, this contribution is very valuable for future modeling activities.

In section 2 the propagation campaign is described. The required stability of interfade duration statistics is also discussed, and the relevance of the available database is stressed. Section 3 presents the interfade duration statistical analysis, and in section 4 the main conclusions are drawn.

2. Propagation Experiment and Statistical Stability of Interfade Duration

2.1. Description of the Propagation Campaign

The propagation campaign was carried out in Aveiro, Portugal, which according to the Köppen-Geiger climate classification is characterized for experiencing a temperate Mediterranean climate (Csb), but oceanic climate (Cfb) influences are present due to the coastal geographical location of Aveiro and the Atlantic Ocean [*Oak Ridge National Laboratory Distributed Active Archive Center*, 2013; *Peel et al*., 2007]. The experiment took almost 9 years, starting on September 2004 and ended on July 2013, after the Eutelsat 13A satellite has been repositioned.

The propagation measurements, with sampling rate of one sample per second, are characterized by an availability higher than 99.9%. The 0.1% of out of service is due to short maintenance periods in clear-sky conditions, so we assume that the interfade events are not interrupted during out of service periods; this assumption is reasonable especially for attenuation thresholds above 1 dB. They include 8 years and 10 months (hereinafter referred to as 9 years period for brevity) of in-excess attenuation (dynamic range up to 25 dB, value above which the carrier-to-noise ratio becomes too low to be possible to consider accurate the recorded data at higher attenuations), cross-polarization discrimination, rainfall rate (up to 120 mm/h), wind speed, humidity, and ground temperature.

The main parameters of the satellite campaign and of the link geometry are listed in Table 1.

2.2. Assessment of the Required Statistical Stability

Before proceeding with the analysis, it is important to assess the required statistical stability of the interfade duration that has a great impact on the obtained results and when accessing the relevance of the ones published in the past or to be published in the future in similar climatological regions.

In order to evaluate the statistical stability, several sub–data sets were generated first and are presented in Table 2 where each pair of numbers aa-bb represents the starting and ending year in a compact form. One year of measurements starts on September and ends next August.

The CCCDF was then computed for each sub–data set (short-term CCCDFs) and for the nine consecutive years (long-term CCCDF).

Table 2. Generated Sub–Data Sets

Number of Years (P_x)	Combinations
$x = 1$	04;05;06;07;08;09;10;11;12;13
$x = 2$	04-06;05-07;06-08;07-09;08-10;09-11;10-12;11-13
$x = 3$	04-07;05-08;06-09;07-10;08-11;09-12;10-13
$x = 4$	04-08;05-09;06-10;07-11;08-12;09-13
$x = 5$	04-09;05-10;06-11;07-12;08-13
$x = 6$	04-10;05-11;06-12;07-13
$x = 7$	04-11;05-12;06-13
$x = 8$	04-12;05-13

The natural logarithm of the ratio of probability values of short- and long-term CCCDFs for the attenuation thresholds of 3, 10, and 20 dB has been calculated to evaluate the impact of adding additional years of data according to (1), where P_t represents the probability values of the long-term CCCDF and P_x represents the probability values for each sub–data set.

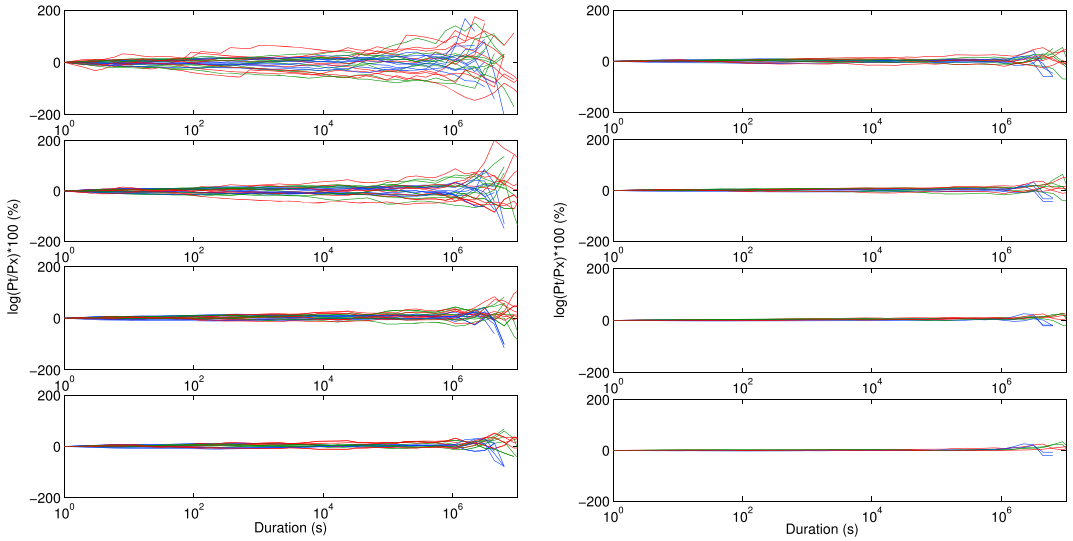

Figure 1. Natural logarithm of the ratio between the long-term CCCDF and each CCCDF obtained using different sub–data sets. Each subplot represents all the results for a given number of years. (left column) The results from (1) obtained using all the possible combinations of $x = 1$ of Table 2 are depicted; (right column) the results from (1) obtained for the sub–data set of $x = 8$. Red lines for the attenuation threshold of 20 dB, green ones for 10 dB, and the blue ones for 3 dB.

$$\varepsilon(d) = \log\left(\frac{P_t(d)}{P_x(d)}\right) \times 100 \tag{1}$$

The results are presented in Figure 1 where each subplot presents all the possible combinations for a given number x of years. The first presents all the combinations for $x = 1$, the second one all the combinations for $x = 2$, and so on up to 8 years.

As it is possible to see, adding successively a greater number of years leads to a convergence of ε and to a decrease on the impact of the natural variability when considering different periods of time.

Similar conclusions can be taken when plotting the probability values for each sub–data set against the long-term values for the attenuation thresholds of 3, 10, and 20 dB, as noticed from Figure 2.

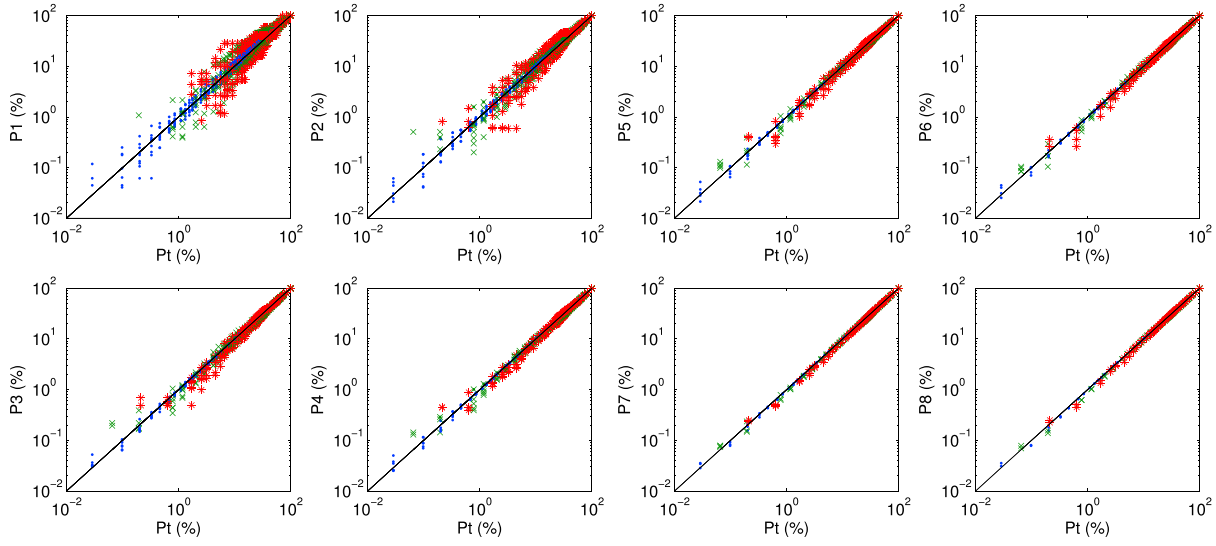

Figure 2. Probability values for each sub–data set against the long-term one. Red stars for the attenuation threshold of 20 dB, green crosses for 10 dB, and the blue dots for 3 dB.

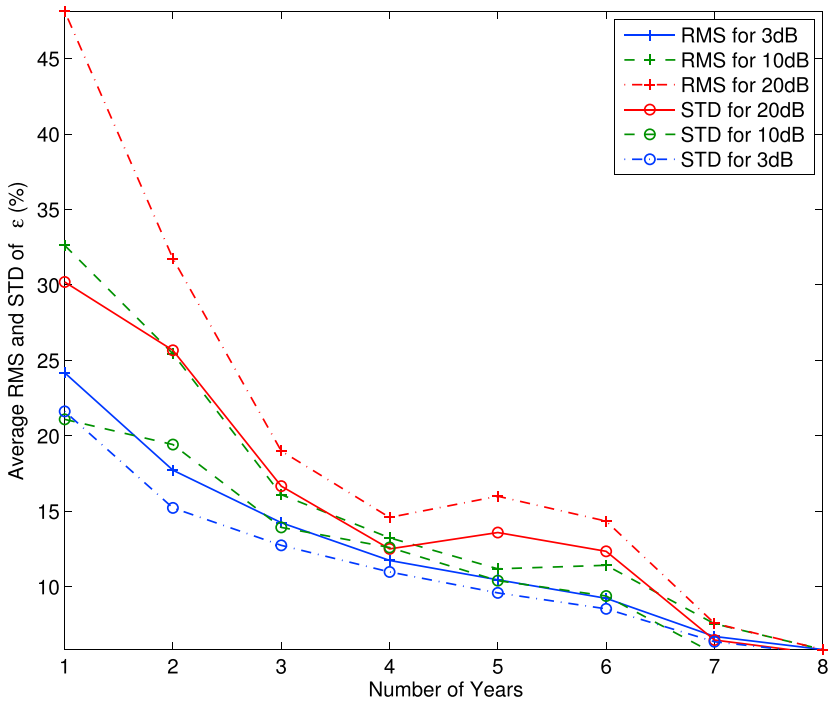

Figure 3. Average root-mean-square and average standard deviation of the error (1) for all the combinations of number of years.

Finally, taking all the combinations for a given period, the average standard deviation and average root-mean-square of (1) are presented in Figure 3 and Table 3, where a decrease is noticed for both as the number of years considered increases.

The RMS and standard deviation (STD) values, for the same combination of years, are higher for higher attenuation thresholds due a reduced number of events in the data set and mainly for a smaller number of years. Also, increasing the number of years beyond six has a limited impact.

3. Interfade Duration Analysis

In this section, we present the characterization of the interfade duration on unfiltered data, so the results include also the scintillation effects.

3.1. Number and Duration of the Interfade Events

We have first calculated the number of interfade events for each attenuation threshold. The results are presented in Figure 4 where it appears evident that the number of events decreases as the attenuation

Table 3. Average Root-Mean-Square and Average Standard Deviation

	Attenuation Thresholds (dB)					
	3		10		20	
Number of Years (P_x)	RMS	SD	RMS	SD	RMS	SD
$x = 1$	24.18	21.62	32.62	21.09	48.14	30.2
$x = 2$	17.72	15.23	25.44	19.42	31.75	25.67
$x = 3$	14.24	12.74	16.10	13.93	19.00	16.67
$x = 4$	11.74	10.98	13.24	12.60	14.60	12.51
$x = 5$	10.46	9.59	11.19	10.41	16.00	13.59
$x = 6$	9.23	8.53	11.42	9.39	14.35	12.34
$x = 7$	6.71	6.36	7.55	5.57	7.57	6.47
$x = 8$	5.84	5.56	5.84	5.56	5.84	5.56

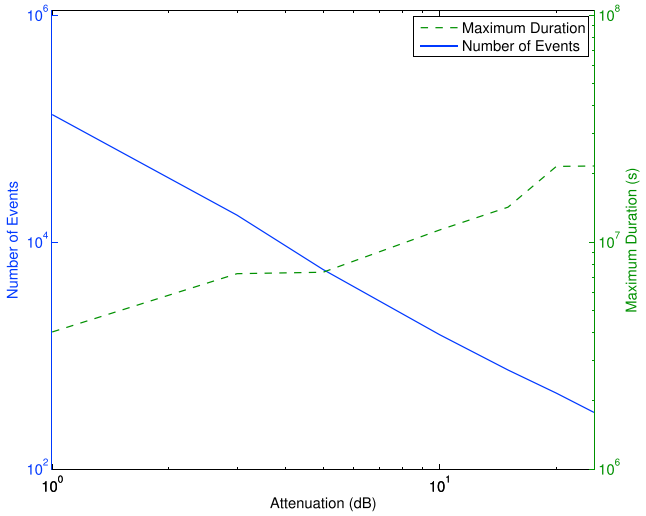

Figure 4. Number of interfade events and the maximum duration observed as a function of the attenuation.

increases and seems to follow a power law distribution. Moreover, the average number of interfade events per year is in Table 4 and as it is possible to see, it drastically decreases as the attenuation threshold increases. For instance, there are on average 15,113 interfade events of 1 dB yr^{-1}, whereas an average of 36 interfade events of 25 dB yr^{-1} is recorded.

In the same figure, we can observe that the maximum duration of the interfade events (green dashed curve) increases, as expected, with the attenuation threshold. For instance, considering an attenuation of 1 dB, the maximum duration observed was about 47 days, while for 25 dB the maximum duration was about 251 days.

As can also be seen in Figure 4, the increase of the maximum duration observed in an interfade event is not regular. The maximum duration seems to be quite similar between 3 and 5 dB and between 20 and 25 dB while a smoother increase is observed for the remaining attenuation thresholds. This information can be useful when considering the best scenario on the arrival process of fade events.

In spite of being large, the maximum duration values presented previously correspond only to extreme events, as the average duration observed for each attenuation threshold is comparatively modest.

In fact, the average duration of interfade events together with the corresponding standard deviation, shown in Figure 5, seems to follow a power law distribution as for the number of interfade events.

The average duration of an interfade event of 1 dB is 34 min, whereas one of 25 dB is about 10 days. From the satellite system's point of view, this information provides the average time between two consecutive outages; it increases with the attenuation threshold. The same behavior is observed for the standard deviation of the time between two consecutive outages, so caution should be taken in systems' design to the time needed to recover from heavy propagation impairments.

Although depending on the attenuation threshold, the exceeded number of seconds is essentially constant up to 28 h, as can be seen in Figure 6. The total interfade time does not increase with the attenuation threshold; rather, it seems to be primarily due to interfade events of 5 dB, followed by the 3 dB, 1 dB, 10 dB, 20 dB, 15 dB, and 25 dB ones. Furthermore, the total interfade time is quite similar for the attenuation thresholds of 1 and 10 dB and 15 and 20 dB. Indeed, both the interfade events of 1 and 10 dB seem to have a similar distribution up to almost 2 min and a similar conclusion can be drawn for the interfade events of 15 and 20 dB up to 28 h.

The histogram of Figure 7 shows the distribution of the number of interfade events; the larger number of events is clearly associated to the lower durations, as expected. In fact, due to scintillation and other small-scale effects, a large number of interfade events should occur for durations up to 30 s as concluded by *Amaya and Nguyen* [2005] and *Braten et al.* [2001]. Furthermore, the interfade events associated to higher attenuation thresholds assume, as expected, a greater range of values for the duration.

Table 4. Average Number of Interfade Events per Year

Attenuation Threshold (dB)	Average Number of Events per Year
1	15,113
3	1,962
5	652
10	173
15	85
20	53
25	36

3.2. Probability Distributions of the Interfade Events

The CCCDF of the number of interfade events is depicted in Figure 8. Clearly,

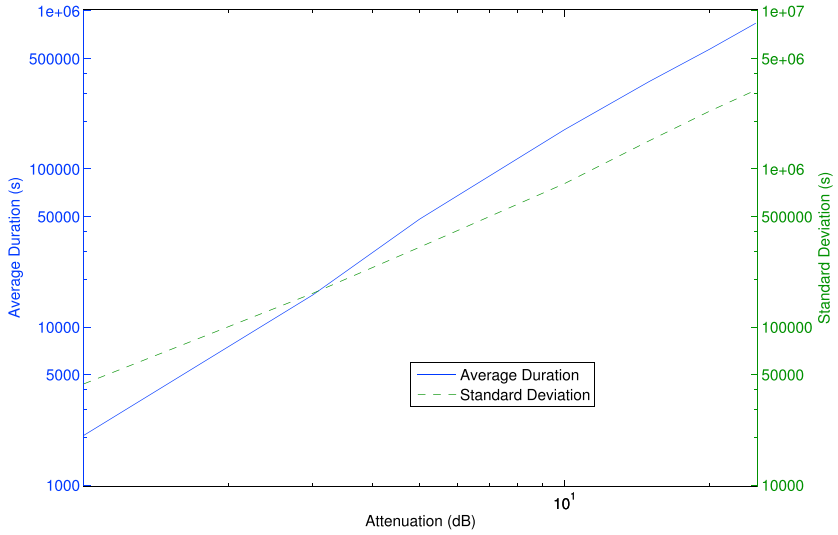

Figure 5. Average duration of interfade events and its standard deviation as a function of the attenuation.

there are a greater number of interfade events for the 1 dB threshold that contribute to 83.6% of the entire database. Interfade events at 3, 5, 10, 15, 20, and 25 dB represent the 10.9, 3.6, 0.96, 0.47, 0.29, and 0.2% of the recorded events, respectively.

Generally, the interfade events at lower attenuation thresholds dominate the distribution; on the contrary, the interfade events at higher attenuations dominate for very long periods starting from a certain duration depending on attenuation. Furthermore, the distribution for higher attenuation thresholds seems to be more constant, while, for lower attenuation thresholds, greater slopes are observed.

The percentage of interfade events exceeding a certain time threshold is also illustrated in Figure 8. More than 50% of the interfade events have durations higher than 3 s and 13% of them have duration longer than 1 min. Moreover, 99% of the interfade events have duration less or equal to 1 day and about 90% of them

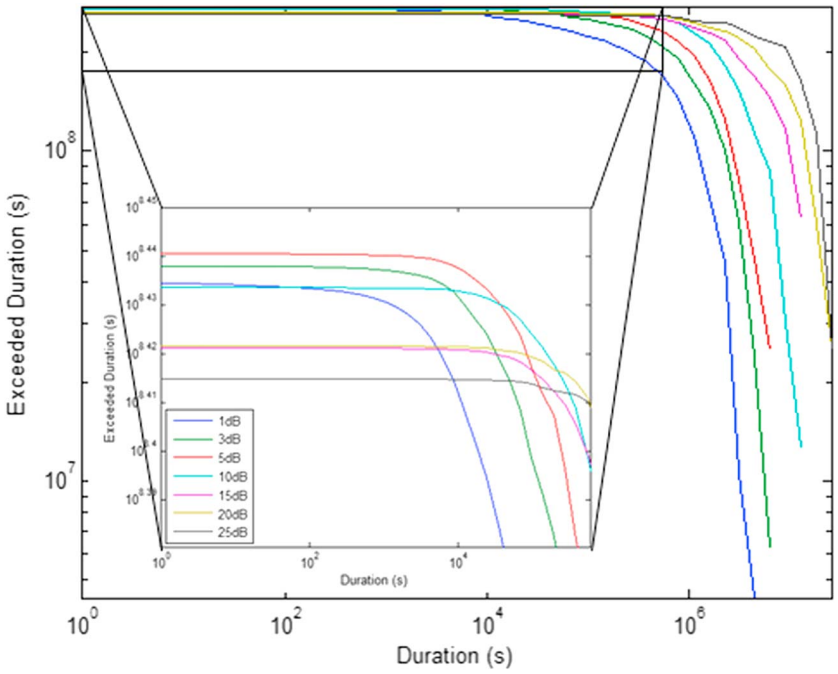

Figure 6. Exceeded time as a function of the duration for the given attenuation thresholds.

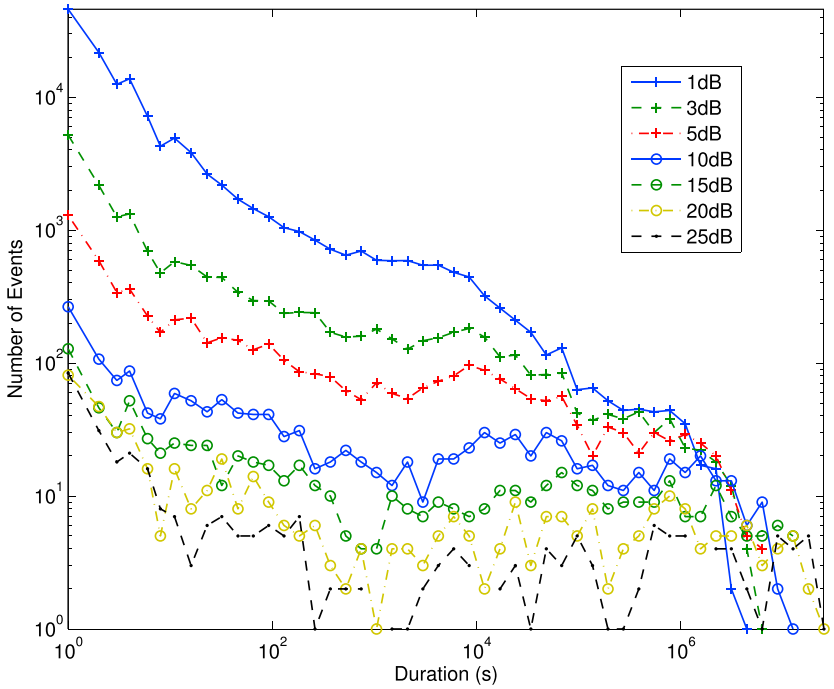

Figure 7. Distribution of the number of interfade events as a function of the duration for the given attenuation thresholds.

have duration less or equal to 130 s, which from the system's point of view means a general high demand for a quick response on recovering after a fade event.

Figure 9 shows the CCCDFs of interfade duration for various attenuation thresholds. They depend on attenuation, as reported in *Amaya and Nguyen* [2005], but their behavior seems to be composed of four distinct phenomena, as it is also evident in Figure 8: scintillation and very short duration events seem to be present up to about 10 s, probably due to the medium microstructure nonhomogeneities (spatial distribution of hydrometeors and their physical properties). Then there is a decrease on the distribution slope up

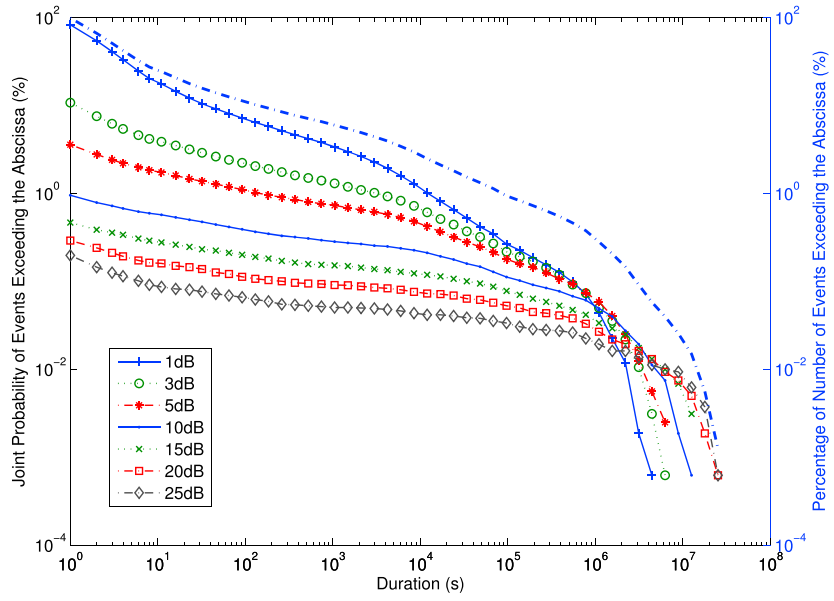

Figure 8. CCCDF of the number of interfade events and total number of events as a function of duration for the given attenuation thresholds.

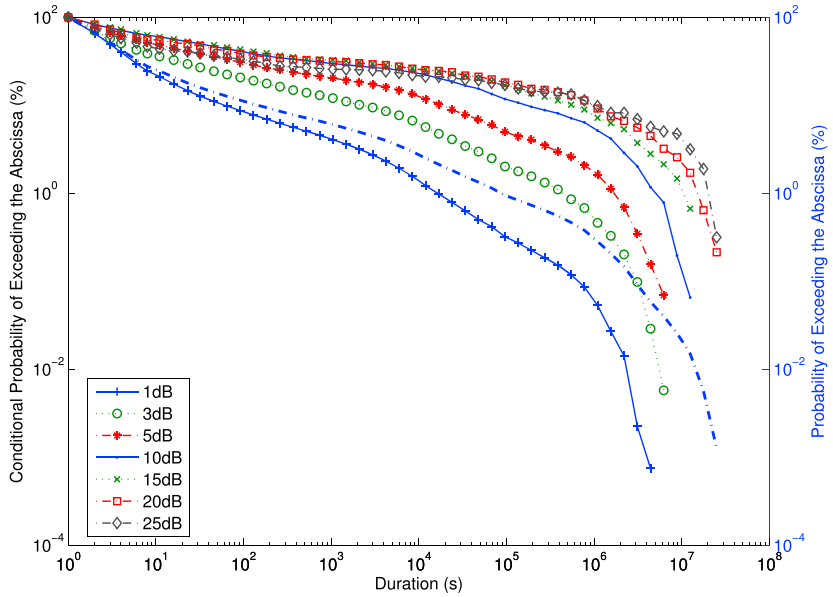

Figure 9. Conditional complementary cumulative distribution function of interfade duration and probability of exceeding the abscissa as function of the duration.

to a duration which depends on the attenuation threshold; this component may be due to the internal rain cells structure like the distribution of the rainfall intensity inside the rain cell. Another increase of the slope is then noticed, probably associated to the rain cells orientation and their horizontal and vertical extent. The final part could be attributed to seasonal phenomena (new rain fronts arriving) and so associated with climate factors.

The interfade duration (to be compared with system recovery time) generally increases with the attenuation, but some caution shall be taken; for instance, there is a probability of about 50% to have an interfade duration longer than 3, 4, 10, 32, 32, 23, and 7 s for attenuation thresholds of 1, 3, 5, 10 15, 20, and 25 dB, respectively.

4. Conclusions

Given the importance of characterizing the satellite communication systems recovering time after a fade event, an exhaustive analysis was performed based on a database of almost 9 years of data with availability higher than 99.9%.

The statistical stability to be observed in temperate Mediterranean climates (Csb) with oceanic climates (Cfb) influences was evaluated concluding that at least 3 years of measurements are needed to characterize the interfade events.

The number of interfade events decrease with the attenuation threshold, which means the satellite system is more often affected by fade events of lower attenuation depths. On the other hand, the average recovering time increases with the attenuation threshold, but caution should be taken since the distribution of the interfade events with the duration turns to be more spread when the attenuation increases. In fact, despite the fact that the recovering time generally increase with the attenuation, that is not true when considering short durations.

The interfade events of 1 dB comprise almost 84% of the whole database, so the remaining interfade events associated to higher attenuation thresholds only contribute about 16%. More than 85% of the interfade events have duration less than or equal to 1 min, imposing a high demand for a quick response on recovering after a fade event.

An attempt was made to relate this behavior with factors such as the internal structure of the rain cell, the rain fronts, and climatic aspects.

Acknowledgments
The authors would like to acknowledge the European Association on Antennas and Propagation (EurAAP) for granting a short-term scientific mission in which framework this study was carried out and Susana Mota who provided a tool able to extract efficiently the interfade events database. Data are available to the colleagues upon request.

References

Amaya, C., and T. Nguyen (2005), Fade and interfade durations on Earth-space links in temperate and tropical locations, in *International Union of Radio Science-URSI Proceeding GA06*, URSI, New Delhi, India.

Amaya, C., and D. V. Rogers (2003), Analysis of fade duration characteristics based on attenuation measurements in Canada and Southeast Asia, in *Proceedings of COST272—European Union Forum for Cooperative Scientific Research*, COST, NA.

Anon (2005), ITU-R P.1623-1: Prediction method of fade dynamics on Earth-space paths.

Arnold, H. W., D. C. Cox, and H. H. Hoffman (1982), Fade duration and interfade interval statistics measured on a 19-GHz Earth-space path, *IEEE Trans. Commun. Com.*, *30*(1), 265–269, doi:10.1109/TCOM.1982.1095372.

Braten, L., and C. Amaya (2000), Fade duration at Ka-band on a satellite-Earth link in Vancouver: Modeling and comparison with measurements, in *IX Simpósio Brasileiro de Microondas e Optoeletrônica (SBMO'IX)*, NA, João Pessoa, Brazil.

Braten, L. E., C. Amaya, and D. V. Rogers (2001), Fade and inter-fade duration at Ka-band on satellite-Earth links: Modelling and system implications, in *AIAA International Communications Satellite Systems Conference*, NA, Toulouse, France.

Castanet, L., and M. Van de Kamp (2003), Modelling the dynamic properties of the propagation channel.

Garcia-del-Pino, P., J. M. Riera, and A. Benarroch (2011), Fade and interfade duration statistics on an Earth-space link at 50 GHz, *IET Microwaves, Antennas Propag.*, *5*(7), 790–794, doi:10.1049/iet-map.2010.0345.

Luglio, M., R. Mancini, C. Riva, A. Paraboni, and F. Barbaliscia (2002), Large-scale site diversity for satellite communication networks, *Int. J. Satell. Commun.*, *20*(4), 251–260, doi:10.1002/sat.723.

Nebuloni, R., L. Rasteghini, C. Riva, M. Luccini, C. Capsoni, A. Martellucci, and G. Piero (2013), Presentation of the analysis tool for design of onboard reconfigurable antenna for broadband SatCom and broadcast services, *Int. J. Artif. Intell. Educ.*, *22*(2–4), 91–98, doi:10.3233/SC-130005.

Oak Ridge National Laboratory Distributed Active Archive Center (2013), FLUXNET maps & graphics web page, from ORNL DAAC, Oak Ridge, Tenn. [Available at http://fluxnet.ornl.gov/maps-graphics.]

Pan, Q. W., and J. E. Allnutt (2004), 12-GHz fade durations and intervals in the tropics, *IEEE Trans. Antennas Propag.*, *52*(3), 693–701, doi:10.1109/TAP.2004.825483.

Paraboni, A., C. Capsoni, G. Masini, J. P. V. P. Baptista, and C. Riva (2002), Dynamic fade restoration in Ka-band satellite systems, *Int. J. Satell. Commun.*, *20*(4), 283–291, doi:10.1002/sat.725.

Paraboni, A., M. Buti, C. Capsoni, D. Ferraro, C. Riva, A. Martellucci, and P. Gabellini (2009), Meteorology-driven optimum control of a multibeam antenna in satellite telecommunications, *IEEE Trans. Antennas Propag.*, *57*(2), 508–519, doi:10.1109/TAP.2008.2011238.

Peel, M. C., B. L. Finlayson, and T. A. McMahon (2007), Updated world map of the Köppen-Geiger climate classification, *Hydrol. Earth Syst. Sci.*, *11*, 1633–1644, doi:10.5194/hess-11-1633-2007.

Timothy, K. I., N. C. Mondal, and S. K. Sarkar (1998), Dynamics properties of rainfall for performance assessment of Earth/space communication links at Ku and Ka bands, *Int. J. Satell. Commun.*, *16*, 53–57, doi:10.1002/(SICI)1099-1247(199801/02)16:1<53::AID-SAT594>3.0.CO;2-H.

Timothy, K. I., J. T. Ong, and E. B. L. Choo (2000), Fade and non-fade duration statistics for Earth-space satellite link in Ku-band, *Electron. Lett.*, *36*(10), 894–895, doi:10.1049/el:20000677.